

Membrane Pores Induced by Magainin[†]

Steve J. Ludtke, Ke He, William T. Heller, Thad A. Harroun, Lin Yang, and Huey W. Huang*

Physics Department, Rice University, Houston, Texas 77005-1892

Received August 15, 1996[⊗]

ABSTRACT: Magainin, found in the skin of *Xenopus laevis*, belongs to a broad class of antimicrobial peptides which kill bacteria by permeabilizing the cytoplasmic membrane but do not lyse eukaryotic cells. The 23-residue peptide has been shown to form an amphiphilic helix when associated with membranes. However, its molecular mechanism of action has been controversial. Oriented circular dichroism has detected helical magainin oriented perpendicular to the plane of the membrane at high peptide concentrations, but Raman, fluorescence, differential scanning calorimetry, and NMR all indicate that the peptide is associated with the head groups of the lipid bilayer. Here we show that neutron in-plane scattering detects pores formed by magainin 2 in membranes only when a substantial fraction of the peptide is oriented perpendicular to the membrane. The pores are almost twice as large as the alamethicin pores. On the basis of the in-plane scattering data, we propose a toroidal (or wormhole) model, which differs from the barrel-stave model of alamethicin in that the lipid bends back on itself like the inside of a torus. The bending requires a lateral expansion in the head group region of the bilayer. Magainin monomers play the role of fillers in the expansion region thereby stabilizing the pore. This molecular configuration is consistent with all published magainin data.

Magainins are 23-residue peptides secreted by the skin of the African clawed frog *Xenopus laevis*. They protect the frog from infection and exhibit a broad-spectrum antibacterial, antifungal, and tumoricidal activities (Zasloff, 1987; Cruciani et al., 1991). Magainins belong to a class of small, antimicrobial peptides which are integral parts of innate immune systems found throughout the animal kingdom (Boman et al., 1994). Related antibacterial peptides have also been found in neutrophils and macrophages (Ganz et al., 1985; Lehrer et al., 1993). By now it is well established that the vast majority of antibacterial peptides act by disrupting cell membranes rather than by interacting with specific protein targets (Lehrer et al., 1993; Boman et al., 1994). However, in most cases the detailed molecular mechanisms of the antibiotic action are still unknown. Magainin adopts a primarily α -helical secondary-structure upon binding to membranes, as determined by CD¹ (Matsuzaki et al., 1989), Raman (Williams et al., 1990), and solid-state NMR (Bechinger et al., 1993). On the basis of its sequence, the helix is hydrophobic along one side parallel to the axis and hydrophilic along the other. Despite this system's apparent simplicity, the molecular mechanism of peptide/membrane interactions is still controversial. Magainin dissipates the membrane potential of biomembranes

(Westerhoff et al., 1989a,b; Juretic et al., 1994), causes leakage from vesicles (Matsuzaki et al., 1989, 1991), induces ion channel activities across lipid bilayers (Duclohier et al., 1989; Cruciani et al., 1991), and has been detected oriented perpendicular to the bilayer at high concentrations (Ludtke et al., 1994). However, NMR (Bechinger et al., 1991, 1992; Hirsh et al., 1996), Raman (Williams et al., 1990), fluorescence (Matsuzaki et al., 1994), and DSC (Matsuzaki et al., 1991) measurements all indicate that the peptide is associated with the head groups of the lipid bilayer and does not significantly disturb the chain region. In this paper we report a neutron in-plane scattering measurement of magainin 2, Gly-Ile-Gly-Lys-Phe²-Leu-His-Ser-Ala-Lys¹⁰-Lys-Phe-Gly-Lys-Ala¹⁵-Phe-Val-Gly-Glu-Ile²⁰-Met-Asn-Ser. The result suggests that magainin forms toroidal pores in the membranes. This model is consistent with all of the previous experiments.

A variety of experiments have shown conclusively that magainin interacts directly with the lipid bilayer rather than with a specific protein target within the membrane. Perhaps the most convincing of these is that all D-enantiomer and the natural L-magainin 2 have the same lytic properties against a variety of Gram-positive and Gram-negative bacteria (Wade et al., 1990; Bessalle et al., 1990). Conductivity measurements in lipid bilayers showed that the pair produced the same current flow. The resistance of red cells to lysis was also similar between the pair. CD showed that the enantiomer formed an exact mirror image of the natural peptide. Presumably this reversal of helical direction would inhibit any protein specific interactions.

Many of the investigations of magainin's molecular mechanism have centered on the orientation of the peptide relative to the plane of the lipid bilayer. Previous OCD measurements have shown that peptide orientation depends on the amount of peptide bound to the membrane (Ludtke et al., 1994). At low peptide concentrations (expressed as the peptide to lipid molar ratio, *P/L*), the helices lie parallel

[†] This work was supported in part by the National Institutes of Health Grant AI34367 and Biophysics Training Grant GM08280; by the Department of Energy Grant DE-FG03-93ER61565; and by the Robert A. Welch Foundation. The facility at the IPNS, National Argonne Laboratory, is funded by the Department of Energy, BES-Materials Science, under Contract W-31-109-Eng-38.

* To whom correspondence should be addressed. Tel: (713) 527-4899. FAX: (713) 527-9033. E-mail: Huang@ion.rice.edu.

[⊗] Abstract published in *Advance ACS Abstracts*, October 15, 1996.

¹ Abbreviations: CD, circular dichroism; OCD, oriented circular dichroism; DSC, differential scanning calorimetry; DMPC, 1,2-dimyristoyl-*sn*-glycero-3-phosphatidylcholine; DMPG, 1,2-dimyristoyl-*sn*-glycero-3-phosphatidylglycerol; POPC, 1-palmitoyl-2-oleoyl-*sn*-glycero-3-phosphatidylcholine; TFE, trifluoroethanol.

to the membrane surface. This result is consistent with all other measurements, including a solid-state NMR measurement of ^{15}N -labeled magainin oriented in multilamellar membranes (Bechinger et al., 1991; 1992). However, for P/L above $\sim 1/30$ a substantial fraction of the bound peptide reorients itself perpendicular to the plane of the lipid bilayer. So far this has only been detected by OCD (Ludtke et al., 1994), and has apparently contradicted other measurements which concluded that the peptide is parallel to the membrane surface even at high concentrations. This apparent contradiction will be resolved by the model presented in the discussion of this paper. However, first we should make clear exactly what was measured in each experiment. In the OCD experiment (Ludtke et al., 1994), the samples consisted of oriented lipid multilayers containing various amounts of peptide. By measuring the UV CD spectrum the orientation of α -helices can be determined quite accurately under a variety of sample conditions (Wu et al., 1990). Our previously published results showed that magainin begins to insert perpendicularly to some membranes as the P/L ratio is raised above $1/30$. These data have since been verified and refined. In particular, we found that insertion depends on the lipid composition of the membrane (unpublished experiments). In the Raman study (Williams et al., 1990), the spectrum of the lipid acyl-chain C–C stretching region was used to indicate the extent of acyl-chain disorder induced by bound peptides. Magainin appeared to be less disrupting than melittin to the acyl chains. DSC measured the effect of magainins on the gel to liquid crystalline phase transition of multilamellar vesicles (Matsuzaki et al., 1991). At 3.5 mol % the effect of magainin to DPPG's main transition seemed insignificant, leading to the conclusion that magainin does not penetrate deeply into the chain region. Fluorescence quenching by lipid quenchers was used to estimate the depth of Trp residues substituted at the 5th, 12th, or 16th position of magainin 2 (Matsuzaki et al., 1994). All Trp residues appeared to be 8–10 Å from the bilayer center, independent of P/L . Most recently solid-state NMR was used to estimate the distance between ^{13}C labels in magainin and the phosphorus in the phospholipid head group, and it was concluded that the helical peptide is in close proximity to the head groups (Hirsh et al., 1996). In short, all of the high peptide concentration experiments, with the exception of OCD, detected the association of magainin with the lipid head groups and assumed that the peptide lies parallel to the bilayer surface. We will show that this last assumption is not justified in this case.

In-plane neutron scattering (He et al., 1995, 1996) detects structures within the membrane where neutron scattering-length densities are higher or lower than that of a pure lipid bilayer. In particular, use of D_2O causes water filled pores within the membrane to stand out in the lipid background.

MATERIALS AND METHODS

Magainin 2 amide was a gift of Drs. M. Zasloff and W. L. Maloy of Magainin Pharmaceuticals, Inc. (Plymouth Meeting, PA). The purity was $>98\%$ by both HPLC and capillary zone electrophoresis. 1,2-Dimyristoyl-*sn*-glycero-3-phosphatidylcholine (DMPC), 1,2-dimyristoyl-*sn*-glycero-3-phosphatidylglycerol (DMPG), and 1-palmitoyl-2-oleoyl-*sn*-glycero-3-phosphatidylcholine (POPC) in CHCl_3 were purchased from Avanti Polar Lipids, Inc. (Alabaster, AL). The lipids were of $>99\%$ purity. Both peptide and lipid

were used without further purification. Lipid was mixed with the appropriate amount of magainin in TFE to produce the desired P/L ratio. The final batches of sample totaled roughly 40 mg each. The solvent was evaporated first under nitrogen and then in vacuum. Next, a few milliliters of H_2O or D_2O were added to the sample, and it was homogenized in a glass homogenizer or by a sonicator. The homogenized sample was then returned to the glass bottle where it was quick-frozen in a dry-ice/ethanol bath. The ice was then slowly evaporated in a freeze-drier over a period of 2–3 days. The resulting sample was fluffy, appearing somewhat like sticky cotton, and occupied a volume 2 orders of magnitude larger than the condensed sample. The bottle was then incubated in a sealed glass jar with D_2O for ~ 2 weeks. This process hydrated the sample from vapor until a clear gel remained at the bottom of the bottle.

The helical orientation of magainin with respect to the plane of the membrane was measured using oriented circular dichroism as described in Wu et al. (1990). Briefly, a small amount of the sample was spread between two quartz plates. The alignment of the lipid multilayers was monitored by polarized microscopy (Huang and Olah, 1987), and then OCD measurements were made on a Jasco J-500 spectropolarimeter with light incident normal to the quartz plates. The OCD spectrum was decomposed into a linear combination of the parallel and the perpendicular magainin spectra (Ludtke et al., 1994), from which the percent of perpendicular orientation was determined. Magainin in DMPC/PG (3:1) at $P/L = 1/10$ showed that 50–80% of the peptide was oriented perpendicular to the membrane surface. This is somewhat less insertion than we reported in earlier experiments (Ludtke et al., 1994) where 80–100% insertion was observed. We should point out that while there are still unknown parameters which are affecting the amount of insertion, we have performed this experiment dozens of times and we consistently see a large degree of insertion at high concentration and no insertion at low concentrations. This variation in the percent of perpendicular orientation will be discussed in detail in a future publication. At $P/L = 1/20$ in DMPC/PG (3:1) the percent of perpendicular orientation was 30–50%. However, at the same concentration magainin in POPC shows 0% insertion. These measurements were performed at $\sim 28^\circ\text{C}$. At 35°C the percent of perpendicular orientation either did not change or showed a slight (up to 10%) decrease in all samples.

Neutron samples were prepared as described in He et al. (1996). Seven thin layers of each hydrated peptide/lipid mixture, each weighing about 5–6 mg, were held between eight parallel quartz plates. The total thickness of the sample was ~ 0.25 mm, and the diameter was ~ 15 mm. The multilayers were aligned by slowly disturbing the whole stack (Huang & Olah, 1987) followed by allowing the stack to sit undisturbed for a few days. Alignment in samples like this has been found to spontaneously improve with time. During this process, alignment was monitored with a polarized microscope. It is possible to focus on each layer independently. The number of liquid crystalline defects (oily streaks) was comparable to Figure 1 of He et al. (1996). Finally the assembly was sealed in an aluminum holder with two quartz windows.

Neutron experiment was performed at the Intense Pulsed Neutron Source in Argonne National Laboratory using the small-angle diffractometer. In-plane scattering was measured

in the transmission mode with neutron incident normal to the multilayer surface and scattered at angle 2θ . For $\theta < 10^\circ$, the momentum transfer, \mathbf{q} (its magnitude = $4\pi \sin \theta/\lambda$), is nearly parallel to the plane of the multilayers. The details of the neutron in-plane scattering technique are described in He et al. (1996).

RESULTS

Figure 1 shows neutron in-plane scattering of a magainin sample in DMPC/PG (3:1) $P/L = 1/20$, measured repeatedly at 25, 29, and 35 °C to test its stability. Each curve consists of a sharp peak and a relatively broader peak. The sharp peak moves from $q \approx 0.09 \text{ \AA}^{-1}$ at 25 °C to $q \approx 0.11 \text{ \AA}^{-1}$ at 29 and 35 °C, whereas the broader peak remains at $q \approx 0.08 \text{ \AA}^{-1}$ for all temperatures. We have shown in previous papers (He et al., 1995, 1996) that the sharp peak is due to lamellar diffraction from liquid crystalline defects (called oily streaks) of the multilayers. Pure lipid samples containing no peptide produce only this sharp peak. This peak can be easily separated from the remaining data using a simple Gaussian fit and provides the repeat spacing, $D = 2\pi/q$, of the sample *in situ*. From lamellar X-ray diffraction experiments, this number can be directly related to the hydration of the sample (Ludtke et al., 1995). The broader peak centered at $q \approx 0.08 \text{ \AA}^{-1}$ is caused by the presence of magainin.

The scans shown in Figure 1 were not in any particular order. They were taken randomly over a period of four days. Despite this, the measurements at 35 °C were very consistent. Even after raising or lowering temperature, the data at 35 °C were reproduced quite well. At 29 °C there is noticeably more variation, and at 25 °C the curve is noticeably different. As the temperature decreases the repeat spacing increases. It is well-known that the D spacing of DMPC increases from the liquid crystalline phase to the gel phase [e.g., Janiak et al. (1976) and Zhang et al. (1995)]. For DMPC/PG this transition is normally at 23 °C. It appears that the presence of a large amount of magainin is causing this transition to broaden and (possibly) shift. This behavior has also been seen in other experiments (Morrow & Davis, 1988). At 29 °C the sample is most likely in some sort of transition state where hysteresis produces significant variations in the measured curve. At 25 °C the sample was clearly in the gel phase: it appeared wax-like and the whole body was birefringent under polarized microscopy.

Samples were measured at several magainin concentrations from $P/L = 1/10$ to $1/30$. All of these samples produced nearly identical scattering curves. There were small variations in the position of the magainin peak, but there was no consistent relation between peak position and magainin concentration. Mean values and variations in parameters obtained by the analyses of these data are discussed later.

The scattering-length densities of DMPC, magainin, H_2O , and D_2O are, respectively, 0.25, 1.48, -0.56 , and 6.35 in the unit of 10^{10} cm^{-2} (Bacon, 1975). The observed neutron scattering is due to variations in scattering-length density within the plane normal to the beam. For example, the lamellar diffraction peak is due to the contrast in the scattering-length density between the alternating layers of D_2O and lipid bilayer in membrane defects where the bilayer surface is tangential to the beam. If the lipid is hydrated with H_2O , the contrast is reduced and the lamellar diffraction by defects becomes so small as to be undetectable (He et

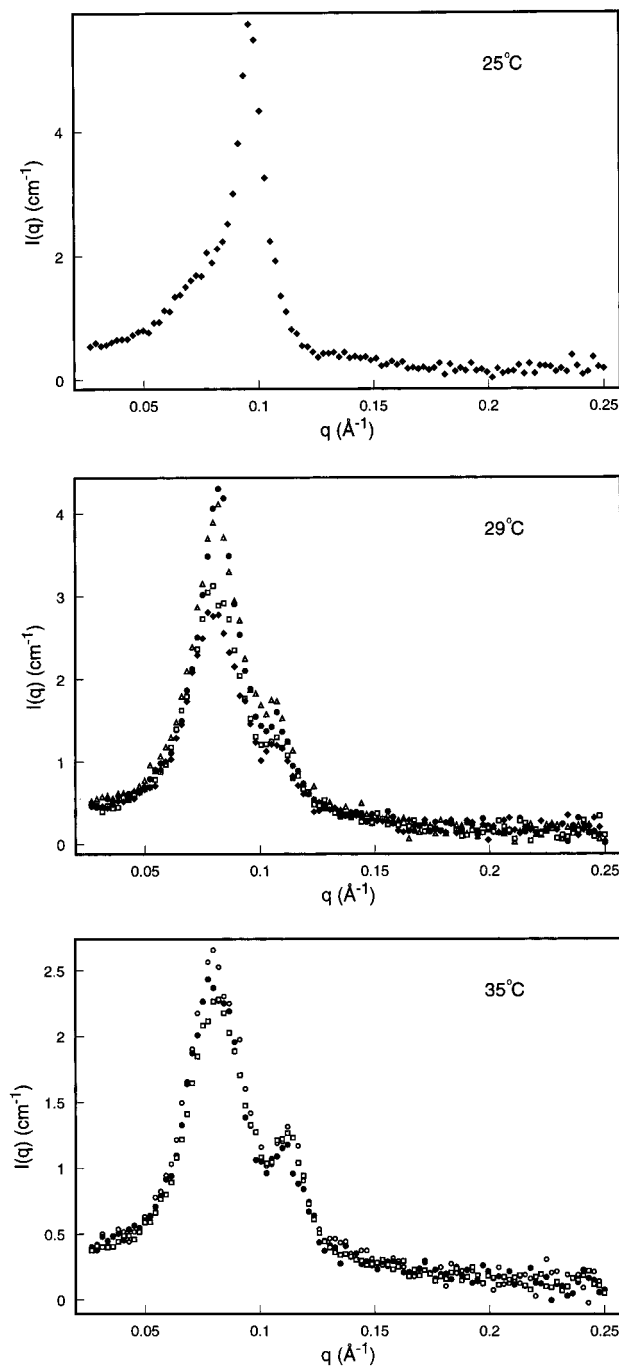


FIGURE 1: Neutron in-plane scattering of DMPC/DMPG (3:1) bilayers containing magainin 2 at the peptide lipid molar ratio $P/L = 1/20$. The same sample was measured repeated and randomly at 25, 29, or 35 °C over a period of 4 days to test its stability. Each scan took about 1 h. Notice that the vertical scale of each panel is different. Each scan consists of a broad peak centered at $q \approx 0.08 \text{ \AA}^{-1}$, which appeared only in the presence of magainin, and a sharp lamellar peak due to liquid crystalline defects in the multilayer sample. The lamellar peak moved with temperature (and hydration, see Figure 2), reflecting different repeat spacings of the multilayers.

al., 1995; 1996). To prove that the magainin peak is primarily due to D_2O associated with the magainin rather than the magainin itself, we exposed a sample initially hydrated with D_2O to H_2O vapor for 24 h. This caused most of the D_2O in the sample to be replaced by H_2O , and consequently the in-plane scattering almost completely disappeared (Figure 2). To insure that the loss of signal was not due to a change in the sample structure, we exchanged the sample back to D_2O and the in-plane scattering reap-

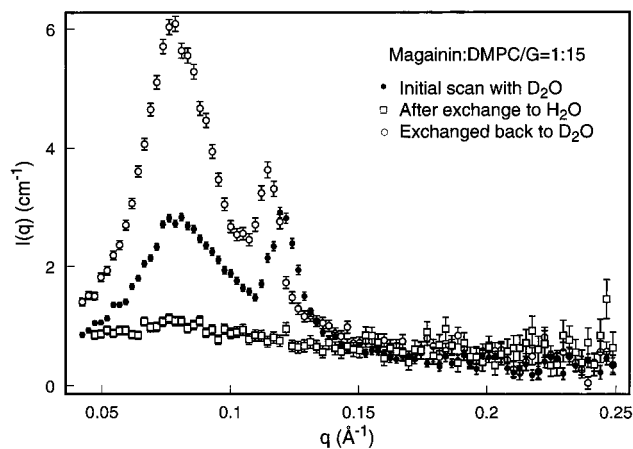


FIGURE 2: Evidence that the pore peak is due almost entirely to the D₂O within the pores. This figure shows the in-plane scattering for magainin in DMPC/DMPG bilayers ($P/L = 1/15$) initially hydrated with D₂O, after the sample was exposed to saturated H₂O vapor for 24 h and subsequently exposed to saturated D₂O vapor for another 24 h. Notice that the lamellar peak shifted between the first and the third scan due to a change in the degree of hydration, but the pore peak remained at the same position in q .

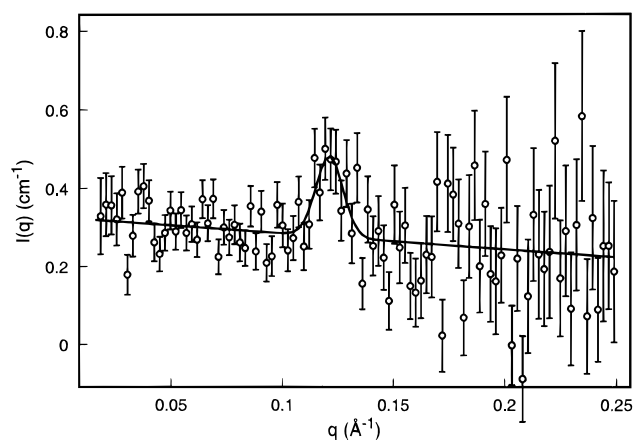


FIGURE 3: Neutron in-plane scattering of POPC bilayers containing magainin at $P/L = 1/20$. Oriented circular dichroism showed that magainin is entirely oriented parallel to the plane of the membrane. The scattering shows only a lamellar peak. (The solid line is a fit.)

peared. This is consistent with the assumption that the in-plane scattering was due to pore-like structures and the scattering was due almost entirely to correlations between the D₂O within the pores. The pore signal was not observed when there were no magainin molecules oriented perpendicular to the plane of the membrane. We prepared a POPC sample contained magainin at $P/L = 1/20$. OCD measurement showed that all the magainin was oriented parallel to the bilayers in this sample, and, as expected, only a lamellar diffraction peak was observed in in-plane scattering (Figure 3).

DISCUSSION

The data were analyzed by the method described in He et al. (1996). Since \mathbf{q} is in the plane of the membrane, one can imagine the whole lipid bilayer being projected onto the plane. We assume that scattering is caused by N identical scattering objects. Then the intensity of neutron in-plane scattering $I(q)$ is given by

$$I(q)/N = |F(q)|^2 S(q) \quad (1)$$

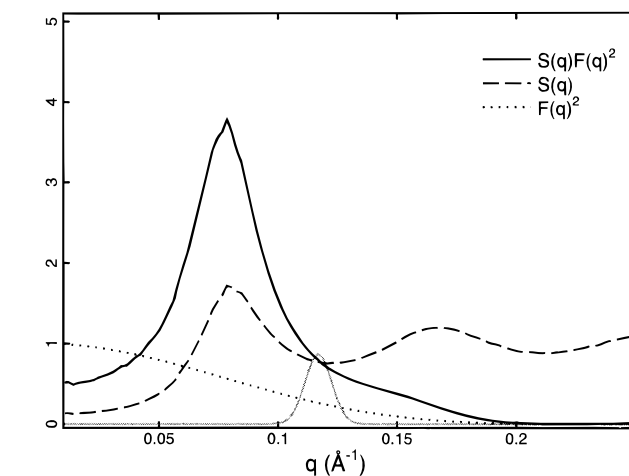
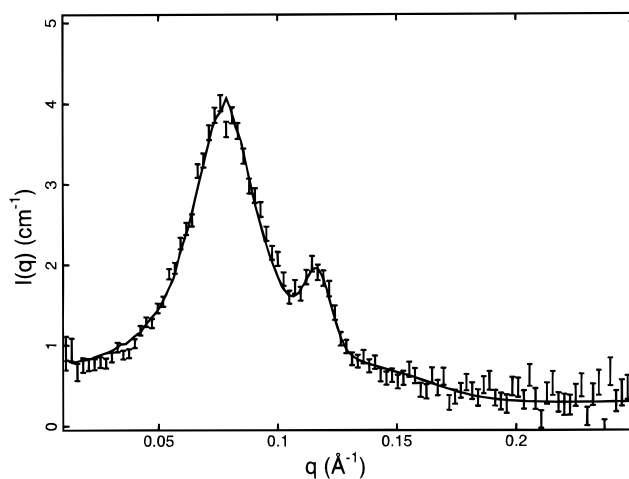


FIGURE 4: Analysis of a representative neutron scattering curve. The sample was magainin 2 in DMPC/DMPG (3:1) bilayers at $P/L = 1/20$. The data was fit with a model $F(q)^2 S(q)$ as described in the text plus a Gaussian for the lamellar peak (the solid line in the top panel). The bottom panel shows the decomposition of the fit: the solid line is the model $F(q)^2 S(q)$ and the gray line is the Gaussian peak. $F(q)^2$ and $S(q)$ are the normalized form factor squared and structure factor, respectively.

The form factor $F(q)$ is the scattering amplitude produced by an individual scattering object. Only the contrast between the scattering object and the lipid background will contribute to the form factor. The structure factor $S(q)$ is the Bessel transform of the correlation function of the scattering objects in the plane of the membrane (He et al., 1993).

To analyze the data, we start with a simple model. Since the form factor is dominated by the contribution of the D₂O in the scattering object, we approximate $F(q)$ by that of a water (D₂O) cylinder of radius r_1 . We assume that the scattering objects are freely diffusing in the plane of the membrane, and the closest approach between two scattering objects is $2R$. R is the contact radius. This was simulated by 1000 circular disks of radius R allowed to randomly diffuse within an area with the restriction that the disks do not overlap with each other (He et al., 1996). The resulting $S(q)$ is a function of the contact radius R and the areal coverage ϕ denoting the fraction of the total area of the plane covered by the disks. With three free parameters r_1 , R , and ϕ , the in-plane scattering curve was fit with eq 1 (Figure 4). Averaging the results from all of the samples gives values of $R = 35.5 \pm 1.5$ Å, $\phi = 46 \pm 2\%$, and $r_1 = 18.5 \pm 1$ Å. For comparison, the in-plane scattering of alamethicin pores

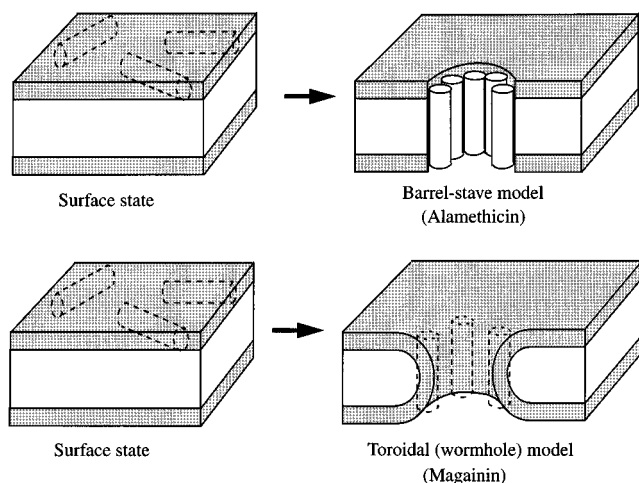


FIGURE 5: Toroidal (or wormhole) model of magainin vs barrel-stave model of alamethicin (the cross sectional view). The small cylinders represent magainin or alamethicin monomers. The shaded area represents the head group region of the lipid bilayer. At low peptide concentrations, both peptides adsorb in the head group region where they lie parallel to the membrane surface. At high peptide concentrations, the free energy of surface adsorption becomes too high, so the peptide is driven to an inserted state. Alamethicin lines a hole in the bilayer by forming a peptide ring. The exterior of the ring contacts the hydrocarbon region of the bilayer in the barrel-stave model. Inserted magainin, on the other hand, remains associated with the head groups. The membrane surface bends in a toroidal fashion to create a pore. Head groups and associated magainin monomers line the pore in the toroidal model.

gave $R \approx 20 \text{ \AA}$ and $r_1 \approx 9 \text{ \AA}$ (He et al., 1995, 1996). The magainin pore is almost twice as large as the alamethicin pore. This has profound implications.

The scattering curve of alamethicin pores fits very nicely with the barrel-stave model (He et al., 1996a). The contact radius $R \approx 20$ matches the total radius of a water cylinder of $r_1 \approx 9 \text{ \AA}$ surrounded by an alamethicin ring of thickness 11 \AA (the diameter of the alamethicin helix). On the contrary, magainin does not fit this model. If we refit the data with a form factor $F(q)$ consisting of a water cylinder of radius r_1 and surrounded by a magainin ring of thickness 11 \AA , R remains the same, $\sim 35.5 \text{ \AA}$, and r_1 becomes even smaller, $\sim 14 \text{ \AA}$. This would make the outside radius of the magainin ring $\sim 25 \text{ \AA}$, which is 10 \AA too small to account for the contact radius. In essence the neutron data require a contact radius about 20 \AA larger than the water core radius. In addition, as shown later, a simple calculation suggests that there are only 4–7 magainin monomers participating in each channel. Barrel-stave channels would require *at least* 11 magainin monomers to form each channel (He et al., 1995). To resolve this conflict, we propose a toroidal (or wormhole) model for the magainin pores (shown schematically in Figure 5). In this model the lipid bilayer bends back on itself like the inside of a torus. This causes the top and bottom monolayers to be continuous. There is an energy cost for such a membrane deformation, mainly due to the bending in the toroidal area. The bending can be viewed as a lateral expansion of the head group region relative to the chains. This strain of expansion would be reduced by the incorporation of magainin monomers in the head group region, thus stabilizing the pore. The length of the peptide would require it to be oriented parallel to the pore axis, agreeing with OCD measurements.

In this model, the number of monomers per pore is determined by the minimum of the membrane deformation energy. On the basis of the areal coverage ϕ and the contact radius R , we estimate that there is one pore per 8370 \AA^2 . Excluding the water hole, this area is occupied by approximately 130 lipids on each monolayer. At $P/L = 1/20$ and 30–50% insertion, we estimate that there are 4–7 magainin monomers present in each pore. Since magainin monomers play the role of “fillers” to relieve the membrane stress, there is probably no peptide–peptide contact, unlike the barrel-stave model. This model gives a contact radius larger than the water core radius by approximately half-a-bilayer thickness (the minor radius of the torus) or about 20 \AA (unpublished X-ray experiments; Lemmich et al., 1995), which is a surprisingly good match to the neutron data. When we fit the data with a form factor of a toroidal model of undetermined size (r_1) and a structure factor of undetermined R , the average result (fits similar to Figure 4) gave $R \approx 35 \text{ \AA}$ and $r_1 \approx 15 \text{ \AA}$.

A similar model was independently proposed by Matsuzaki et al. (1996) to explain their data linking pore formation with the transfer of lipid between the inner and outer membrane leaflets. Here we show that the toroidal model is not only supported by neutron in-plane scattering but also consistent with all previously reported data, in particular magainin monomers are oriented perpendicular to the plane of the membrane while associated with the lipid head groups. The model also predicts no magainin aggregation, consistent with a recent NMR measurement (Hirsh et al., 1996).

The action of magainin is now summarized as follows: At low peptide concentrations, magainin adsorbs in a primarily helical form parallel to the membrane surface, embedded in the head group region. Although the great majority of magainin is on the membrane surface, occasionally a small number of pores are formed as fluctuation phenomena, consistent with the observed ion channel activities (Duclouhier et al., 1989; Juretic et al., 1994) and the leakage experiments (Matsuzaki et al., 1989, 1995, 1996). It is reasonable to assume that such transient pores are similar to the toroidal pores observed at high peptide concentrations. When a pore is closed, the participating magainin monomers will again adsorb in the head group region, but they may surface to either side of the membrane. Thus channel formation provides a mechanism for peptide translocation across the bilayer as observed by Matsuzaki et al. (1995). As shown by Ludtke et al. (1995), the adsorption of magainin in the head group region expands the membrane laterally and consequently decreases the bilayer thickness in proportion to the peptide concentration P/L . Because the energy of membrane deformation is proportional to the square of the thickness change, the energy increases quadratically with the peptide concentration (Huang, 1995). This energy of membrane deformation is part of the free energy of magainin adsorption. Thus at high peptide concentrations, the energy of adsorption may become so high, it drives the lipid–peptide system to other configurations of lower energy. In the case of alamethicin, the surface adsorption state transforms to the insertion state in which alamethicin forms pores in the barrel-stave fashion (He et al., 1996b). Perhaps the difference between alamethicin and magainin is that magainin binds to the head groups more strongly, causing toroidal pores to be the lower energy state.

ACKNOWLEDGMENT

We thank Michael Zasloff and W. Lee Maloy for their generous gift of magainins and thank P. Thiyagarajan and Dennis Wozniak for help with neutron experiments at IPNS.

REFERENCES

- Bacon, G. E. (1975) *Neutron Diffraction*, 3rd ed., Chapter 16, pp 544–580, Clarendon Press, Oxford.
- Bechinger, B., Kim, Y., Chirlian, L. E., Gesell, J., Neumann, J.-M., Motal, M. Tomich, J., Zasloff, M., & Opella, S. J. (1991) *J. Biol. NMR* 1, 167–173.
- Bechinger, B., Zasloff, M., & Opella, S. J. (1992) *Biophys. J.* 62, 12–14.
- Bechinger, B., Zasloff, M., & Opella, S. J. (1993) *Protein Sci.* 2, 2077–2084
- Boman, H. G., Marsh, J., & Goode, J. A., Eds. (1994) *Antimicrobial Peptides*, Ciba Foundation Symposium 186, pp 1–272, John Wiley & Sons, Chichester.
- Cruciani, R. A., Barker, J. L., Zasloff, M., Chen, H.-C., & Colamonici, O. (1991) *Proc. Natl. Acad. Sci. U.S.A.* 88, 3792–3796.
- Duclohier, H., Molle, G., & Spach, G (1989) *Biophys. J.* 56, 1017–1021.
- Ganz, T., Selsted, M. E., Szklarek, D., Harwig, S. S., Daher, K., Bainton, D. F., & Lehrer, R. I. (1985) *J. Clin. Invest.* 76, 1427–1435.
- He, K., Ludtke, S. J., Wu, Y., & Huang, H. W. (1993) *Biophys. J.* 64, 157–162 .
- He, K., Ludtke, S. J., Worcester, D. L., & Huang, H. W. (1995) *Biochemistry* 34, 15614–15618.
- He, K., Ludtke, S. J., Worcester, D. L., & Huang, H. W. (1996a) *Biophys. J.* 70, 2659–2666.
- He, K., Ludtke, S. J., Heller, W. T., & Huang, H. W. (1996b) *Biophys. J.* (in press).
- Hirsh, D. J., Hammer, J., Maloy, W. L., Blazyk, J., & Schaefer, J. (1996) *Biochemistry* (in press).
- Huang, H. W., & Olah, G. A. (1987) *Biophys. J.* 51, 989–992.
- Huang, H. W. (1995) *J. Phys. II (France)* 5, 1427–1431.
- Janiak, M. J., Small, D. M., & Shipley, G. G. (1976) *Biochemistry* 15, 4575–4585.
- Juretic, D., Hendler, R. W., Kamp, F., Caughhey, W. S., Zasloff, M., & Westerhoff, H. V. (1994) *Biochemistry* 33, 4562–4570.
- Lehrer, R. I., Lichtenstein, A. K., & Ganz, T. (1993) *Annu. Rev. Immunol.* 11, 105–128.
- Lemmich, J., Mortensen, K., Ipsen, J. H., Honger, T., Bauer, R., & Mouritsen, O. G. (1995) *Phys. Rev. Lett.* 75, 3958–3961.
- Ludtke, S. J., He, K., Wu, Y., & Huang, H. W. (1994) *Biochim. Biophys. Acta* 1190, 181–184.
- Ludtke, S. J., He, K., & Huang, H. W. (1995) *Biochemistry* 34, 16764–16769.
- Matzuzaki, K., Harada, M., Handa, T., Fumakoshi, S., Fujii, N., Yajima, H., & Miyajima, K. (1989) *Biochim. Biophys. Acta* 981, 130–134.
- Matzuzaki, K., Harada, M., Fumakoshi, S., Fujii, N., & Miyajima, K. (1991) *Biochim. Biophys. Acta* 1063, 162–170.
- Matsuzaki, K., Murase, O., Tokuda, H., Fumakoshi, S., Fujii, N., & Miyajima, K. (1994) *Biochemistry* 33, 3342–3349.
- Matsuzaki, K., Murase, O., Fujii, N., & Miyajima, K. (1995) *Biochemistry* 34, 6521–6526
- Matsuzaki, K., Murase, O., Fujii, N., & Miyajima, K. (1996) *Biochemistry* (in press).
- Morrow, M. R., & Davis, J. H. (1988) *Biophys. J.* 27, 2024–2032.
- Westerhoff, H. V., Juretic, D., Hendler, R. W., & Zasloff, M. (1989a) *Proc. Natl. Acad. Sci. U.S.A.* 85, 910–913.
- Westerhoff, H. V., Hendler, R. W., Zasloff, M., & Juretic, D. (1989b) *Biochim. Biophys. Acta* 975, 361–369.
- Williams, R. W., Starman, R., Taylor, K. M. P., Cable, K., Beeler, T., Zasloff, M., & Covell, D. (1990) *Biochemistry* 29, 4490–4496.
- Wu, Y., Huang, H. W., & Olah, G. A. (1990) *Biophys. J.* 57, 797–806.
- Zasloff, M. (1987) *Proc. Natl. Acad. Sci. U.S.A.* 84, 5449–5453.
- Zhang, R., Sun, W., Tristram-Nagle, S., Headrick, R. L., Suter, R. M., & Nagle, J. F. (1995) *Phys. Rev. Lett.* 74, 2832–2835.

BI9620621